*Limnol. Oceanogr.*, 57(3), 2012, 684–697

doi:10.4319/lo.2012.57.3.0684

# Solubility of iron in the Southern Ocean

Christian Schlosser,[a,b,*] Christina L. De La Rocha,[c,d] Peter Streu,[a] and Peter L. Croot [a,e]

[a] Leibniz Institut für Meereswissenschaften an der Universität Kiel (IFM-GEOMAR) Kiel, Germany
[b] National Oceanography Centre, Southampton, United Kingdom
[c] Alfred-Wegener-Insitut für Polar- und Meeresforschung, Bremerhaven, Germany
[d] Laboratoire des Sciences de l'Environnement Marin (LEMAR), Institut Universitaire Européen de la Mer (IUEM), Université de Bretagne Occidentale, Plouzané, France
[e] Plymouth Marine Laboratory, Plymouth, United Kingdom

*Abstract*

Iron solubility ($cFe_S$) ranged from 0.4 to 1.5 nmol $L^{-1}$, decreasing from south to north in three different Southern Ocean zones (the Coastal Zone, the Antarctic Zone, and the Polar Frontal Zone plus the Subantarctic Zone). This decrease was at times correlated with an increase in temperature. Organic Fe solubility ($cFe_{S,org}$), which was obtained by subtracting from total measured Fe solubility the solubility of inorganic species of iron (Fe) at the measurement temperature (20°C), ranged from 0.3 to 1.3 nmol $L^{-1}$, representing an average of 32 ± 14% of the concentration of ligands in the dissolved size fraction as determined via competitive ligand exchange–absorptive cathodic stripping voltammetry (barring a handful of extremely high values from a transect run to the east of Prydz Bay). Values of $cFe_S$ were mainly lower than the predicted value for inorganic Fe solubility at the in situ temperature. Total in situ Fe solubility ($cFe_{S,adj}$) was therefore estimated by adjusting for inorganic Fe solubility at in situ temperatures (between −2°C and +18°C). Because in situ temperatures in the Antarctic Circumpolar Current were mostly lower than +3°C, such $cFe_{S,adj}$ values, ranging from 0.5 to 1.8 nmol $L^{-1}$, were roughly twice as large as $cFe_{S,org}$. The adjustment relies heavily on model calculations of inorganic Fe solubility but, if correct, indicates that the bulk of the solubility of Fe in the cold waters of the Southern Ocean is tied to the solubility of inorganic Fe rather than to Fe ligands in the soluble size fraction.

The limited availability of the micronutrient iron (Fe) restricts the growth of phytoplankton in what are termed high-nutrient, low-chlorophyll regions, such as the Southern Ocean (Martin 1990; Boyd 2002). The low concentrations of Fe in seawater stem largely from Fe's particle reactive nature under oxic conditions and its thus brief residence time in ocean water (Croot et al. 2004*b*). It has been shown that the capacity of seawater for soluble Fe (Fe solubility; $cFe_S$) and the related stability of soluble Fe species vary with both physical conditions, such as temperature (T) and pH, and with chemical conditions, such as organic ligand concentrations (Kuma et al. 1996; Liu and Millero 2002). Fe solubility experiments are usually conducted by filtering seawater through a 0.02-$\mu$m syringe filter or ultrafiltration membrane and then adding a known amount of radiolabeled Fe, preferably $^{55}Fe$. The total amount of Fe able to pass through the filter membrane is defined as Fe solubility. Gaining insights into how Fe solubility shifts in the ocean related to upwelling, phytoplankton blooms, organic matter remineralization, and other physical and biological factors that influence the composition and concentration of organic ligands is a key part of refining our understanding of the marine biogeochemical cycling of Fe.

In seawater, Fe occurs both in different size fractions and in different chemical forms. Fe in seawater has been operationally defined, via filtration, as occurring in particulate ($Fe_P$; $> 0.2$ $\mu$m) and dissolved ($Fe_D$; $< 0.2$ $\mu$m) size fractions. Dissolved Fe can be further divided into soluble ($Fe_S$; $< 0.02$ $\mu$m) and colloidal ($Fe_C$; 0.02–0.2 $\mu$m) size fractions (Nishioka et al. 2005). Furthermore, Fe in these different size fractions exists in either an inorganic chemical form or bound to an organic ligand.

More than 99% of the dissolved Fe in the ocean is thought to be complexed to Fe-binding ligands (Rue and Bruland 1997; Witter and Luther 1998). These ligands are released during the remineralization of organic matter (Tani et al. 2003; Schlosser and Croot 2009), directly from phytoplankton via viral cell lysis (Gobler et al. 1997) and zooplankton grazing (Sato et al. 2007), or by bacteria under low-Fe conditions (Martinez et al. 2000). Ligands may be released in soluble and colloidal form and may aggregate with each other or with dissolved organic matter (DOM; Schlosser and Croot 2008) and thus occur across continuums of size and binding strength.

Ligand-bound Fe is less particle reactive than inorganic Fe and therefore has a longer residence time in both the soluble and the dissolved size fractions. In the absence of Fe-binding ligands, most of the Fe added to seawater would be quickly converted into the potentially less bioavailable colloidal and particulate forms (Baker and Croot 2010). The concentration of dissolved ligands (0.2-$\mu$m filtered) in open ocean seawater, at 0.5–6 nmol $L^{-1}$ (Croot et al. 2004*a*,*b*), exceeds typical concentrations of dissolved Fe (0.02–0.5 nmol $L^{-1}$), providing excess binding capacity capable of coping with episodic inputs of Fe (Wagener et al. 2008).

Not all the solubility of Fe is due to organic complexation. For example, Fe solubility in seawater exposed to ultraviolet (UV) radiation to destroy DOM and in artificial

* Corresponding author: C.Schlosser@noc.soton.ac.uk

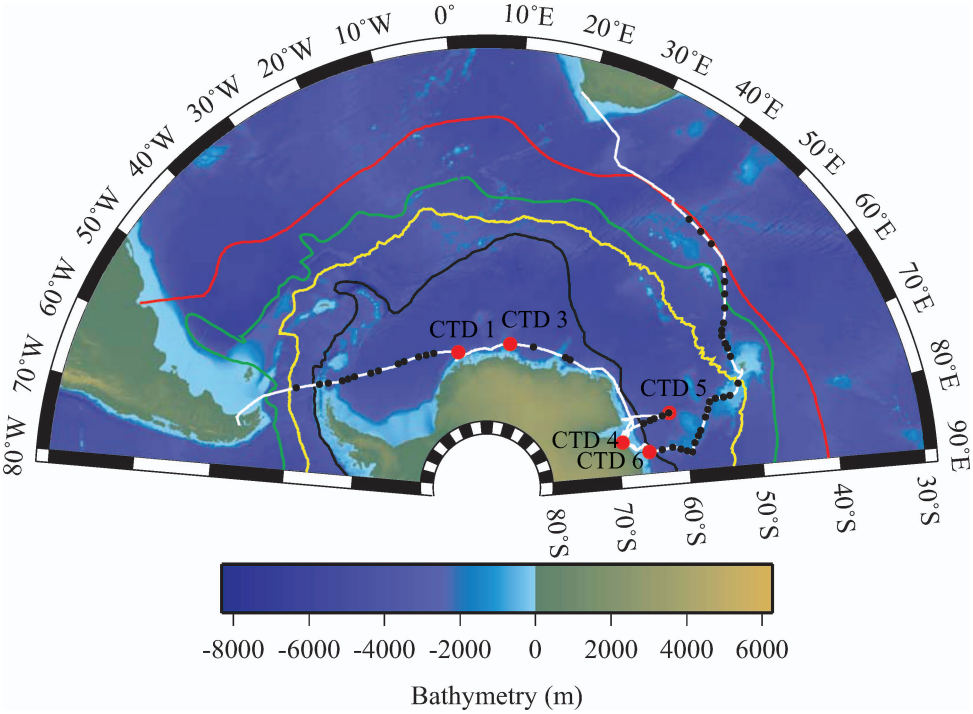


Fig. 1. The cruise track of the R/V *Polarstern* during ANTXXIII/9, moving from Punta Arenas, Chile, in February 2007 to Cape Town, South Africa, in April via the Weddell Sea, Neumeyer Station, Prydz Bay, and the Kerguelen Islands (white line). Small black circles are surface sampling locations (depth ≈ 12 m), and the larger red circles are locations of Niskin rosette casts. Also shown are the Subtropical Front (STF) in red, the Subantarctic Front (SAF) in green, the Polar Front (PF) in yellow, and the Southern Boundary of the Antarctic Circumpolar Current (SBACC) in black.

seawater free from DOM has still been observed to be between 0.01 and 0.15 nmol $L^{-1}$ at 20°C (compared to about 0.5 nmol $L^{-1}$ in untreated seawater; Kuma et al. 1996; Liu and Millero 2002; Schlosser and Croot 2008). The exact contribution of this "inorganic" solubility to total Fe solubility depends on factors such as temperature and pH, with higher values of $cFe_S$ found at lower temperature and pH. This can be explained by a shift in the balance between the two hydrolyzed Fe species, $Fe(OH)_3$ and $Fe(OH)_2^+$, to favor the charged form at lower temperatures due to lower water ion product ($pK_w$) values at these temperatures (Covington et al. 1977) and by the crystalline phase transition of solid Fe phases (X. Liu, F. J. Millero, and M. Micic, unpubl.) with different solubility products. Assuming that the same solid Fe phase with the same size distribution exists over the temperature and pH ranges, inorganic Fe solubility can be modeled based solely on salinity, pH, and temperature (Liu and Millero 2002) and provides an inorganic Fe solubility of 0.155 nmol $L^{-1}$ at 20°C and pH 7.8.

Measurements of total Fe solubility can be used to gain a picture of the cycling of soluble organic ligands in the ocean. For example, Nakabayashi et al. (2002) found a positive linear correlation of nitrate plus nitrite ($NO_x$) concentrations and Fe solubility in the water column, and Schlosser and Croot (2009) found linear correlations between $cFe_S$ and phosphate, pH, and apparent oxygen utilization. These and other results have indicated that soluble organic ligands can be produced during the decomposition of organic matter by microbes, either through the release of ligands by actively growing microbes or by the release or activation of soluble ligands from organic matter during the decomposition process (Boyd et al. 2010).

In order to further our understanding of the processes linking Fe solubility and biological activity, we undertook measurements of Fe solubility and Fe ligand concentrations during the R/V *Polarstern* expedition ANTXXIII/9 over a broad temporal and geographic range of the Southern Ocean (Fig. 1). With these data, we aim to examine the links between Fe solubility and dissolved Fe-binding ligand concentrations, temperature, and nutrient regeneration.

## Methods

*Description of the study area*—The majority of the data reported here come from samples collected within the Antarctic Circumpolar Current (ACC). The ACC moves an enormous volume of water from west to east around the Antarctic continent and is driven by the prevailing westerly winds (Tomczak and Godfrey 2003). It is bounded to the north by the Subtropical Front (STF) and to the south by the Southern Boundary of the ACC (SBACC). In places such as (but not limited to) the Drake Passage, its path is tightly constrained by topography (Tomczak and Godfrey

2003). Interaction between the ACC and the Antarctic continent gives rise to a large clockwise-rotating gyre in the Weddell Sea aptly named the Weddell Gyre.

The ACC can be divided into several widely recognized circumpolar zones characterized by differences in salinity and temperature (Brown et al. 1989; Tomczak and Godfrey 2003). The Subantarctic Zone falls between the STF and the Subantarctic Front (SAF). The Polar Frontal Zone lies between the SAF and the Polar Front (PF). The Antarctic Zone exists between the PF and the SBACC. South of the SBACC (and thus also of the ACC) lies the Coastal Zone.

Together, Antarctic Bottom Water (ABW) and North Atlantic Deep Water (NADW) that was transported from the northern hemisphere to the Southern Ocean form Antarctic Circumpolar Water (ACW). This water rises to the surface at the Antarctic Divergence (Brown et al. 1989). Some of this water will flow poleward, eventually sinking to become ABW. The upwelled water that flows northward from the Antarctic Divergence will sink at the Antarctic Convergence in the Polar Frontal Zone to form Antarctic Intermediate Water.

*Sampling and first treatment*—The expedition ANTXXIII/9 (Fig. 1) took place on the R/V *Polarstern* between February and April 2007 in the Atlantic and Indian sector of the Southern Ocean. Surface water samples collected during ANTXXIII/9 stretched from the Coastal Zone of Antarctica to the Subtropical Front (Fig. 1). In addition to these 53 surface samples, there were five deep-water stations (Niskin rosette) from which seawater for measurements of Fe solubility ($cFe_S$) and nutrient concentrations were made on water from depths of 20, 40, 60, 80, 200, and 500 m.

The surface seawater samples were collected using a "snorkel" with a Teflon nose (Helmers et al. 1991). This snorkel was deployed through the "moon pool" in the hull of the ship and thus extended 2 m beneath the vessel keel and took up seawater from 12 m below the sea surface. When the vessel was steaming at a velocity of at least 6 kn, seawater was pumped on board through Teflon-coated polyethylene tubing by a Teflon diaphragm pump (Almatec A-15 TTT). Part of this water was pumped, unfiltered, directly into a clean polyethylene carboy, while the remainder was passed through a 0.2-$\mu$m in-line Sartorius cartridge filter. Subsamples of the filtered seawater were dispensed into acid-cleaned low-density polyethylene (LDPE) sample bottles under clean air conditions (clean bench).

Profiles of the upper 500 m of the water column were collected using non–trace metal clean Niskin bottles deployed on a conventional water sampling rosette. These samples were filtered through a 0.2-$\mu$m membrane filter (Sartorius) and dispensed into acid-cleaned LDPE bottles (Nalgene).

Samples for Fe solubility were either set up immediately for measurement (as described below) or stored briefly at $-20^{\circ}$C. The 0.2-$\mu$m filtered seawater for dissolved trace metal analysis (Fe, zinc, cadmium, cobalt, copper, manganese, titanium, lead, and nickel) was acidified with quartz-distilled nitric acid to pH 1.8, stored in the dark at room temperature, and then measured a few months later under clean lab conditions by graphite furnace–atomic absorption spectrometry at the Leibniz Institute für Meereswissenschaften (IFM-GEOMAR) in Kiel, Germany, by a method previously outlined by Danielsson et al. (1978) and Bruland et al. (1979) and described in detailed in chapter 12.2 in the textbook of Grasshoff et al. (1999). Fe ligand samples were transferred immediately into a $-20^{\circ}$C freezer and shipped frozen to the IFM-GEOMAR, for analysis (described below).

Nutrient samples were filtered through 0.6-$\mu$m polycarbonate filters, dispensed into LDPE bottles, and frozen immediately at $-20^{\circ}$C for analysis at the Alfred-Wegener-Institut in Bremerhaven, Germany. The polycarbonate filters were immediately frozen and stored at $-80^{\circ}$C for later determination of chlorophyll *a* (Chl *a*) content in Bremerhaven. Phosphate was measured via an autoanalyzer (Technicon ASM II) using the method of Grasshoff et al. (1999). Chl *a* concentrations were measured on a fluorometer (Turner Designs TD-700), following extraction in the dark in acetone at $-20^{\circ}$C.

*Sample treatment: Fe solubility*—Fe solubility measurements were performed using the radioisotope $^{55}$Fe (received from Hartmann Analytics, Braunschweig, Germany). The $^{55}$Fe solution had a specific activity of 157.6 MBq mg$^{-1}$ Fe and a total activity of 75 MBq and was dissolved in 0.1 mol L$^{-1}$ HCl. Further dilutions were produced using 18 megaΩ-cm deionized water (reverse osmosis prefeed UV oxidation Milli-Q; MQ) and were acidified with quartz-distilled hydrochloric acid (Q-HCl) to pH 1.8.

The experimental setup for the measurement of Fe solubility was adapted from Kuma et al. (1996) and Nakabayashi et al. (2002) and is described in full in Schlosser and Croot (2009). After the addition of $^{55}$Fe in the seawater sample to an initial total Fe concentration of $\sim$ 20 nmol L$^{-1}$ at $t_0$ (pH 7.8–8), about 10 mL of the sample were filtered through 0.02-$\mu$m Anotop syringe filters that had been first flushed and then filled with MQ water. The first 6–7 mL of the filtrate were rejected to avoid dead volume artifacts. The remaining 1–2 mL of seawater were filtered into a 60-mL acid-cleaned Teflon bottle and acidified with Q-HCl to avoid wall-sorption effects.

Duplicate 400 $\mu$L of the filtered samples were then taken and transferred into 6-mL scintillation counting vials to which 4.5 mL of counting cocktail (Lumagel Plus®) were added. The same procedure was repeated for subsamples taken at 3, 6, 24, 48, and 72 h. After filtration and cocktail addition, the closed vials were then placed in a liquid scintillation counter (Packard, Tri-Carb 2900TR) and counted for at least 30 min. Throughout all of this, the samples were handled at room temperature ($\sim$ 20$^{\circ}$C) and stored in the dark. The average of Fe solubility measured after 48 and 72 h is the value normally reported for Fe solubility ($cFe_S$).

*Sample treatment: Dissolved Fe-binding ligands*—Determination of the concentrations of total dissolved Fe-binding ligands in the samples was performed using the well-established method of competitive ligand equilibration–adsorptive cathodic stripping voltammetry on a three-

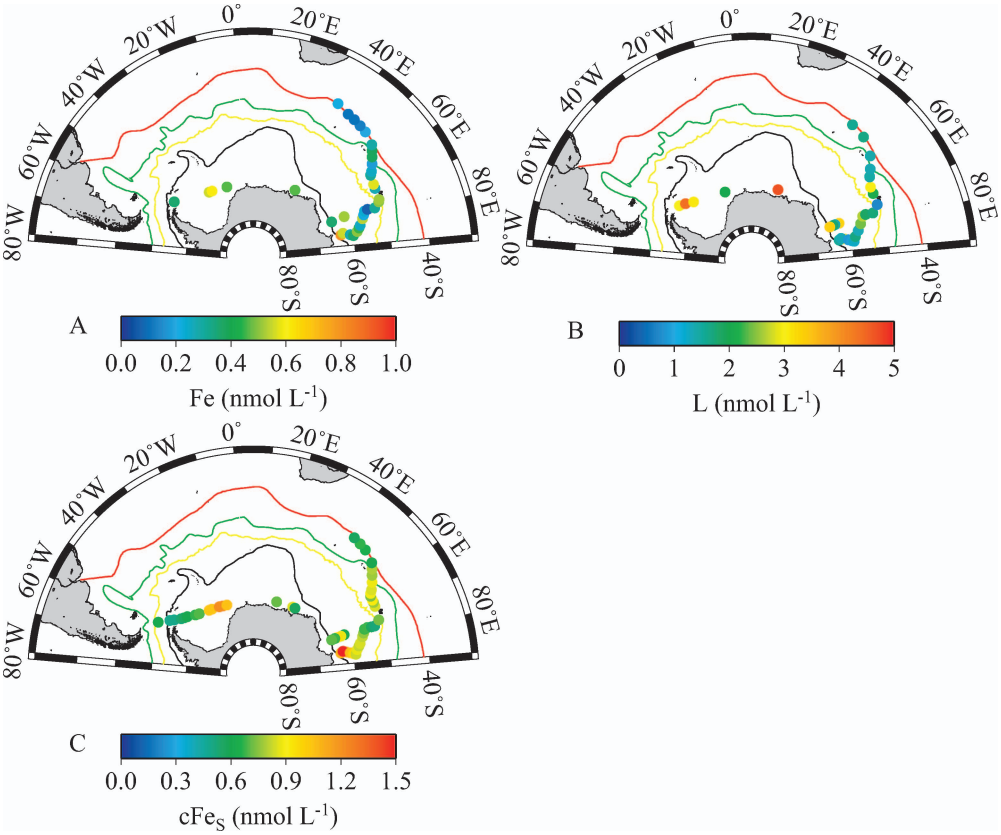


Fig. 2. (A) Dissolved Fe, (B) total dissolved ligands, and (C) Fe solubility ($cFe_S$) in surface seawaters along the cruise track. Also shown are the frontal boarders of the Antarctic Circumpolar Current (same as in Fig. 1).

electrode voltammeter (Metrohm 757 Computrace) using the method of Croot and Johansson (2000). The voltammetric apparatus consisted of a static mercury drop electrode, a double-junction Ag-AgCl reference electrode with a salt bridge filled with 3 mol $L^{-1}$ KCl, and a platinum counter electrode. Fe standards were prepared in MQ; 2-(2-thiazolylazo)-p-cresol (TAC) was used as the competitive ligand and N-(2-hydroxyethyle)piperazine-N′-2-propanesulfonic acid (EPPS) as the buffer to hold seawater at pH 8.0. The TAC solution was prepared in high-performance liquid chromatography–grade methanol and EPPS in MQ with 1 mol $L^{-1}$ ammonium solution ($NH_4OH$) (v : v; 1 : 1). The voltammetric analysis with the competitive ligand method using 0.2-$\mu$m filtered seawater (used for our experiments) was carried out at 4°C by using a conventional water bath connected to a Metrohm quartz glass cup and enabled measurement of the concentration of Fe-complexing ligands in the dissolved size fraction. Note that the total dissolved fraction contains ligands in the soluble and colloidal size fractions, not just those in the soluble fraction.

## Results

*Surface samples*—The highest dissolved Fe concentrations in surface waters (Fig. 2; Table 1) were found at the SBACC near Prydz Bay (~ 0.8 nmol $L^{-1}$), around the Kerguelen plateau (~ 0.6 nmol $L^{-1}$) and in the center of the Weddell Gyre (~ 0.6 nmol $L^{-1}$). The lowest dissolved Fe concentrations were measured between the SBACC and the PF (< 0.2 nmol $L^{-1}$) and in the open ocean between the Kerguelen Plateau and Cape Town (< 0.1 nmol $L^{-1}$).

Measurements of $cFe_S$ in surface samples (Figs. 2, 3) of the Southern Ocean, which were taken during the late austral summer and early austral autumn (February, March, and early April), fell between 0.5 and 0.9 nmol $L^{-1}$ in most areas (i.e., from the Drake Passage through the center of the Weddell gyre, from Prydz Bay (the SBACC) to the Kerguelen Islands (PF), and between the PF and the SAF [from the Kerguelen Plateau to Cape Town]). High $cFe_S$ values (1.0–1.2 nmol $L^{-1}$) occurred between the center of the Weddell Gyre and the edge of the Antarctic ice shelf. A second set of high values (those reaching 1.5 nmol $L^{-1}$) occurred at the edge of the Southern Boundary of the ACC to the east of Prydz Bay.

The highest total dissolved Fe-binding ligand concentrations (3–4.5 nmol $L^{-1}$) did not occur at the same locations as the highest $cFe_S$ values (Figs. 2, 3). The highest ligand concentrations were observed in the western half of the Weddell Gyre and at the Southern Boundary of the ACC near Prydz Bay but to the west of the location where $cFe_S$ peaked.

*Depth profiles*—In general, $cFe_S$ values at 20 m in the depth profiles were higher than the values at 500 m (Fig. 4;

Table 1. Parameters measured for surface and water column samples from ANTXXIII/9.

| No. | Date 2007 | Position | | Water depth (m) | Sample depth (m) | T (°C) | $PO_4$ ($\mu$mol $L^{-1}$) | Chl *a* ($\mu$g $L^{-1}$) | DFe (nmol $L^{-1}$) | L (nmol $L^{-1}$) | $cFe_S$ (nmol $L^{-1}$) |
|---|---|---|---|---|---|---|---|---|---|---|---|
| | | Latitude | Longitude | | | | | | | | |
| 1 | 05 Feb | −57.45 | −58.47 | 3890 | 12 | 3.45 | 1.69 | 0.06 | | | 0.61±0.03 |
| 2 | 05 Feb | −61.07 | −53.34 | 1683 | 12 | 0.26 | 1.93 | 1.69 | | | 0.48±0.01 |
| 3 | 05 Feb | −62.03 | −51.68 | 3143 | 12 | 0.40 | 1.71 | 0.50 | 0.36 | | 0.49±0.03 |
| 4 | 06 Feb | −63.46 | −48.54 | 3419 | 12 | 0.10 | 1.74 | | | 2.99±0.11 | 0.53±0.01 |
| 5 | 06 Feb | −63.95 | −46.97 | 3832 | 12 | −0.44 | 1.65 | 0.08 | | | 0.56±0.16 |
| 6 | 06 Feb | −64.51 | −45.12 | 4541 | 12 | −0.02 | 1.47 | 0.25 | | 4.38±0.06 | 0.61±0.11 |
| 7 | 07 Feb | −65.89 | −40.43 | 4587 | 12 | 0.31 | 1.75 | 0.09 | | 3.08±0.12 | 0.67±0.09 |
| 8 | 07 Feb | −66.39 | −37.96 | 4660 | 12 | 0.08 | 1.83 | 0.07 | | | 0.70±0.00 |
| 9 | 08 Feb | −67.48 | −30.59 | 4659 | 12 | −0.21 | 1.96 | 0.07 | 0.56 | | 1.03±0.03 |
| 10 | 08 Feb | −67.66 | −28.35 | 4724 | 12 | −0.02 | 1.91 | 0.11 | 0.61 | | 1.04±0.07 |
| 11 | 09 Feb | −68.12 | −22.50 | 4903 | 12 | 0.07 | 1.69 | 0.50 | | | 1.21±0.04 |
| 12 | 09 Feb | −68.34 | −19.60 | 4877 | 12 | −0.09 | 1.66 | 0.59 | | | 1.21±0.05 |
| 13 | 09 Feb | −68.58 | −16.50 | 4864 | 12 | −0.06 | 1.63 | 0.22 | 0.47 | 2.03±0.08 | 1.05±0.20 |
| CTD 1 | 11 Feb | −69.40 | −7.00 | 2972 | 20 | −0.84 | | | | | 0.60±0.06 |
| | | | | | 40 | −1.52 | | | | | 0.55±0.05 |
| | | | | | 60 | −1.66 | | | | | 0.50±0.01 |
| | | | | | 80 | −1.72 | | | | | 0.49±0.04 |
| | | | | | 200 | −1.15 | | | | | 0.57±0.01 |
| | | | | | 500 | 0.70 | | | | | 0.88±0.07 |
| CTD 3 | 16 Feb | −68.42 | 14.17 | 3408 | 20 | 0.33 | 1.54 | 0.32 | | | 0.83±0.05 |
| | | | | | 40 | −0.26 | 1.83 | 0.58 | | | 0.70±0.01 |
| | | | | | 60 | −1.68 | 1.93 | | | | 0.52±0.01 |
| | | | | | 80 | −1.77 | 2.00 | 0.10 | | | 0.55±0.03 |
| | | | | | 200 | −1.19 | 2.06 | 0.06 | | | 0.59±0.02 |
| | | | | | 500 | 0.82 | 2.15 | 0.32 | | | 0.52±0.01 |
| 14 | 17 Feb | −68.03 | 23.46 | 4036 | 12 | −0.02 | 1.42 | 0.28 | | | 0.71±0.03 |
| 14b | 17 Feb | −67.93 | 25.87 | 3830 | 12 | | 1.65 | 0.18 | | 4.65±0.07 | |
| 15 | 18 Feb | −67.48 | 36.26 | 3306 | 12 | 0.24 | 1.91 | 0.10 | | | 0.86±0.05 |
| 16 | 18 Feb | −67.39 | 38.24 | 4214 | 12 | −0.12 | 1.91 | 0.12 | 0.47 | | 0.57±0.19 |
| CTD 4 | 24 Feb | −68.72 | 70.68 | 825 | 20 | −0.11 | 0.98 | 3.55 | | | 0.65±0.05 |
| | | | | | 40 | −0.48 | 1.71 | 0.61 | | | 0.67±0.02 |
| | | | | | 60 | −1.10 | 1.94 | 0.45 | | | 0.69±0.01 |
| | | | | | 80 | −1.41 | 2.05 | 0.22 | | | 0.62±0.00 |
| | | | | | 200 | −1.85 | 2.14 | 0.08 | | | 0.57±0.00 |
| | | | | | 500 | −1.96 | 2.18 | 0.26 | | | 0.44±0.02 |
| CTD 5 | 02 Mar | −60.95 | 72.72 | 4162 | 20 | 0.80 | 1.68 | 0.23 | | | 0.62±0.01 |
| | | | | | 40 | 0.79 | 1.71 | 0.25 | | | 0.60±0.02 |
| | | | | | 60 | −0.62 | 2.08 | 0.19 | | | 0.64±0.01 |
| | | | | | 80 | 1.24 | 2.12 | 0.08 | | | 0.62±0.01 |
| | | | | | 200 | 1.71 | 2.46 | | | | 0.73±0.01 |
| | | | | | 500 | 2.00 | 2.31 | | | | 0.59±0.01 |
| 17 | 03 Mar | −61.03 | 72.72 | 4190 | 12 | 0.86 | 1.70 | 0.21 | 0.52 | | 0.60±0.06 |
| 18 | 03 Mar | −62.06 | 72.72 | 4068 | 12 | 0.87 | 1.56 | 0.91 | | 3.30±0.12 | 0.87±0.07 |
| 19 | 04 Mar | −63.28 | 72.72 | 3952 | 12 | 0.67 | 1.57 | 1.50 | | 1.36±0.07 | 0.96±0.03 |
| 20 | 04 Mar | −63.97 | 72.72 | 3733 | 12 | 0.14 | 1.85 | 0.09 | | 1.78±0.10 | 0.67±0.07 |
| 21 | 05 Mar | −64.96 | 72.72 | 3424 | 12 | 0.22 | 1.68 | 0.83 | 0.36 | 3.34±2.10 | 0.70±0.01 |
| 22 | 18 Mar | −63.54 | 82.83 | 2836 | 12 | 0.30 | 1.59 | 0.24 | | 1.17±0.10 | 1.06±0.05 |
| 23 | 19 Mar | −61.98 | 82.83 | 2440 | 12 | 0.55 | 1.73 | 0.09 | | 2.80±0.14 | 1.12±0.02 |
| CTD 6 | 21 Mar | −65.35 | 82.67 | 3079 | 20 | −1.67 | 1.75 | 0.23 | | | 0.76±0.05 |
| | | | | | 40 | −1.41 | 1.75 | 0.25 | | | 0.63±0.01 |
| | | | | | 60 | −1.24 | 1.83 | 0.19 | | | 0.67±0.03 |
| | | | | | 80 | −1.49 | 1.92 | 0.08 | | | 0.60±0.00 |
| | | | | | 200 | −1.60 | 2.09 | | | | 0.57±0.01 |
| | | | | | 500 | 0.72 | 2.11 | | | | 0.69±0.01 |
| 24 | 22 Mar | −63.52 | 82.83 | 2804 | 12 | 0.25 | 1.56 | 0.22 | 0.81 | 1.52±0.02 | 1.08±0.02 |
| 25 | 22 Mar | −62.84 | 82.09 | 2302 | 12 | 0.53 | 1.69 | 0.32 | 0.56 | 1.34±0.04 | 1.50±0.01 |
| 26 | 23 Mar | −60.88 | 83.74 | 1718 | 12 | 0.71 | 1.68 | 0.07 | 0.27 | 0.85±0.02 | 1.06±0.04 |
| 27 | 23 Mar | −60.02 | 84.64 | 2042 | 12 | 0.28 | 1.65 | 0.12 | 0.36 | 0.92±0.01 | 0.98±0.05 |
| 28 | 24 Mar | −59.38 | 85.19 | 4435 | 12 | 0.08 | 1.60 | 0.15 | 0.97 | 1.25±0.06 | 0.83±0.02 |

Table 1. Continued.

| No. | Date 2007 | Position | | Water depth (m) | Sample depth (m) | T (°C) | $PO_4$ ($\mu$mol $L^{-1}$) | Chl *a* ($\mu$g $L^{-1}$) | DFe (nmol $L^{-1}$) | L (nmol $L^{-1}$) | $cFe_S$ (nmol $L^{-1}$) |
|---|---|---|---|---|---|---|---|---|---|---|---|
| | | Latitude | Longitude | | | | | | | | |
| 29 | 25 Mar | −58.76 | 82.86 | 2022 | 12 | 0.98 | 1.76 | 0.12 | 0.50 | 1.67±0.01 | 0.87±0.01 |
| 30 | 25 Mar | −58.08 | 81.30 | 1753 | 12 | 1.14 | 1.81 | 0.13 | 0.45 | | 0.82±0.04 |
| 31 | 25 Mar | −57.57 | 80.14 | 1752 | 12 | 1.28 | 1.68 | 0.10 | 0.25 | 1.34±0.03 | 0.84±0.01 |
| 32 | 26 Mar | −56.42 | 77.15 | 2429 | 12 | 1.41 | 1.77 | 0.12 | 0.54 | 2.42±0.14 | 0.82±0.00 |
| 33 | 26 Mar | −55.81 | 75.50 | 3016 | 12 | 1.55 | 1.67 | 0.06 | 0.22 | | 0.76±0.02 |
| 34 | 26 Mar | −55.22 | 73.92 | 2229 | 12 | 2.61 | 1.74 | 0.18 | 0.23 | 2.66±0.18 | 0.67±0.03 |
| 35 | 27 Mar | −54.25 | 73.66 | 2079 | 12 | 2.41 | 1.71 | 0.16 | 0.08 | 1.84±0.13 | 0.68±0.04 |
| 36 | 27 Mar | −53.18 | 74.13 | 265 | 12 | 3.15 | 1.70 | 0.36 | | | 0.56±0.02 |
| 37 | 27 Mar | −52.30 | 74.26 | 256 | 12 | 3.08 | 1.82 | 0.54 | 0.30 | 1.72±0.10 | 0.52±0.01 |
| 38 | 28 Mar | −50.68 | 72.47 | 555 | 12 | 3.91 | 1.70 | 1.26 | 0.50 | | 0.73±0.01 |
| 38b | 28 Mar | −50.35 | 71.65 | 650 | 12 | | 1.61 | 0.29 | 0.52 | 0.71±0.02 | |
| 39 | 30 Mar | −50.04 | 66.67 | 2292 | 12 | 4.16 | 1.63 | 0.21 | 0.27 | 2.10±0.07 | 0.85±0.01 |
| 40 | 30 Mar | −49.88 | 64.92 | 287 | 12 | 4.63 | 1.66 | 0.23 | 0.58 | | 0.77±0.03 |
| 41 | 30 Mar | −49.79 | 63.88 | 719 | 12 | 5.19 | 1.62 | 0.20 | | 3.03±0.14 | 0.91±0.01 |
| 42 | 31 Mar | −49.63 | 62.15 | 4061 | 12 | 5.42 | 1.56 | 0.10 | 0.97 | | 0.74±0.02 |
| 43 | 31 Mar | −49.23 | 61.20 | 2765 | 12 | 5.93 | | | 0.30 | | 0.89±0.02 |
| 44 | 31 Mar | −48.56 | 60.21 | 4449 | 12 | 6.22 | 1.51 | 0.12 | 0.25 | 1.44±0.04 | 0.85±0.03 |
| 45 | 01 Apr | −47.24 | 57.96 | 4487 | 12 | 7.92 | 1.23 | 0.28 | 0.18 | 1.36±0.13 | 0.88±0.00 |
| 46 | 01 Apr | −46.11 | 55.91 | 4187 | 12 | 8.13 | 1.29 | 0.40 | 0.38 | | 0.78±0.01 |
| 47 | 02 Apr | −45.11 | 54.13 | 3641 | 12 | 6.94 | 1.34 | 0.28 | 0.38 | 1.40±0.12 | 0.79±0.03 |
| 48 | 02 Apr | −44.11 | 52.39 | 3443 | 12 | 9.59 | 1.21 | 0.30 | 0.29 | | 0.60±0.02 |
| 49 | 03 Apr | −42.96 | 47.71 | 3132 | 12 | 11.82 | 1.17 | 0.20 | 0.20 | 1.65±0.12 | 0.64±0.05 |
| 50 | 04 Apr | −42.67 | 44.86 | 3164 | 12 | 13.50 | 1.13 | 0.19 | 0.13 | | 0.67±0.00 |
| 51 | 05 Apr | −42.39 | 42.07 | 3562 | 12 | 17.61 | 0.44 | 0.51 | 0.11 | 1.57±0.04 | 0.56±0.02 |

Table 1). In three of the five profiles, $cFe_S$ decreased with depth from 20 m down to 80 m. Fe solubility at the site furthest offshore and situated over the deepest seafloor (CTD 5) showed little variation with depth, remaining, one high value aside, within 0.03 nmol $L^{-1}$ of an average value of 0.61 nmol $L^{-1}$. Sta. 5 was also marked by a deeper wind-driven mixed layer than the other more shoreward sites. Sta. 6, occurring late in the season when sea ice was beginning to reform and the water column to overturn, had no surface mixed layer at all. These samples were collected from a non–trace metal clean Niskin rosette, and thus dissolved Fe concentrations were not measured. Because of this, the Fe solubility results shown have not been corrected for in situ Fe and therefore slightly underestimate Fe solubility (i.e., by $< 20$ pmol $L^{-1}$). However, the order of magnitude greater amount of $^{55}Fe$ added (20 nmol $L^{-1}$) during the solubility measurement prevents the in situ dissolved Fe from having much of an influence on the estimation of Fe solubility.

## Discussion

*Patterns of $cFe_S$ in surface waters of the Weddell Sea and the Kerguelen Plateau*—One surprising feature of Fe solubility is that it decreased from south to north in the Coastal Zone, the Antarctic Zone, and the Polar Frontal Zone (Fig. 3A; Table 1). In the Weddell Sea (where all samples were from south of the SBACC), $cFe_S$ shifted from 1.2 nmol $L^{-1}$ at the edge of the shelf ice (samples 12 and 13) to 0.48 nmol $L^{-1}$ near the Drake Passage (sample 2). On the Kerguelen Plateau (Antarctic Zone), $cFe_S$ decreased from 1.50 nmol $L^{-1}$ at the SBACC (sample 25) to 0.52 nmol $L^{-1}$ at the PF (sample 37). Values also declined, although less dramatically (i.e., from about 0.9 to 0.6 nmol $L^{-1}$), between the PF and the STF (samples 41–51).

It is not clear what has caused the above patterns in the different zones, nor even that they have a similar root cause. This is revealed by a closer look at samples 13 to 2 (from the Weddell Gyre) and samples 25 to 37 (the Antarctic Zone samples from the Kerguelen Plateau). While $cFe_S$ in both samples sets declined coherently and dramatically from south to north (Fig. 5A), only the Kerguelen Plateau samples also showed a dramatic decrease in $cFe_S$ with increasing in situ temperature (Fig. 5B). In any event, the samples from the Weddell Gyre did not show a relationship with temperature, suggesting that latitudinal trends have a stronger effect on the $cFe_S$ surface values observed.

The decrease in $cFe_S$ is especially strong between the PF and SBACC and south of the SBACC. This might be explained as net loss of soluble ligands in surface waters over time away from frontal regions, where there is perhaps net production of soluble ligands associated with high levels of biological activity (Gobler et al. 1997; Martinez et al. 2000; Sato et al. 2007). For example, high values of $cFe_S$ in waters near the edge of the ice shelf in the Weddell Sea around 20°W and 68°S (samples 11–13) coincide with elevated concentrations of Chl *a* (Fig. 3; Table 1). This surface water would have been then moved by the Weddell Gyre across the Weddell Basin toward the northern tip of the Antarctica Peninsula (Orsi et al. 1993). Since there was

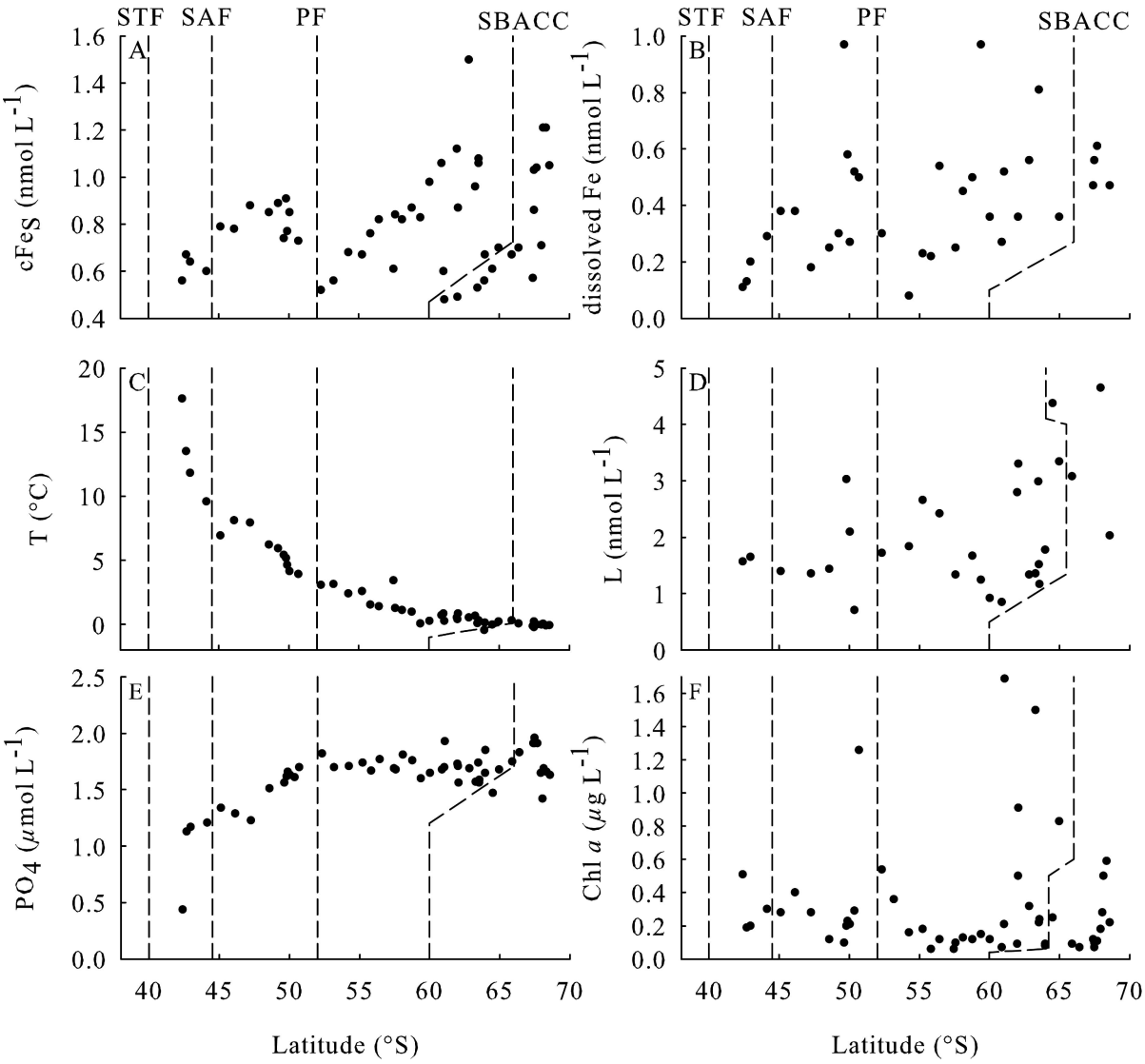


Fig. 3. Data from the surface samples: (A) $cFe_S$, (B) dissolved Fe, (C) temperature, (D) dissolved ligand concentration, (E) phosphate, and (F) Chl *a*. Dashed lines indicate the different Antarctic fronts between 40°S and 70°S (Subtropical Front [STF] at 40°S, Subantarctic Front [SAF] at 45°S, Polar Front [PF] at 52°S, and Southern Boundary of the ACC [SBACC] at 60°C [Weddell Sea] and 65°S [Prydz Bay]).

no further notable net biological activity in this direction (Chl *a* concentrations declined northward, while phosphate concentrations did not), losses of soluble ligands due to exposure to UV radiation (Barbeau 2006) or to consumption by phytoplankton or bacteria (Phinney and Bruland 1994; Shaked et al. 2005) may have been unmatched by the production of new ligands, causing the observed decrease in Fe solubility.

Something similar could have occurred between the SBACC east of Prydz Bay and the PF. Here as well, surface waters would have been driven northward (Heil and Allison 1999), in this case through a combination of wind and the Coriolis effect (Tomczak and Godfrey 2003). This water was a mixture of NADW and ABW, known as ACW, that rose to the surface at the Antarctic divergence, which in this area occurred near the SBACC (Smith et al. 1984). It may be that this freshly upwelled water spurred the growth of phytoplankton and bacteria or brought with it higher concentrations of Fe ligands in the soluble size fraction due to the production or release of ligands in association with organic matter remineralization (Schlosser and Croot 2009). There was no significant change in phosphate concentrations between the SBACC and the PF (Fig. 3E), and, for the most part, Chl *a* concentrations remained low from about 63°S up to the PF after a set of high values near the SBACC (Fig. 3F), indicating perhaps a lack of sufficient biological activity to maintain high concentrations of ligands in the soluble phase as this water spent an increasing amount of time at the surface.

There is a main inconsistency with this hypothesis for the northward declines in Fe solubility that should be noted. This is that $cFe_S$ is not supported by the measurements of Fe ligand concentrations in the dissolved phase; concentrations of the dissolved ligands may have declined

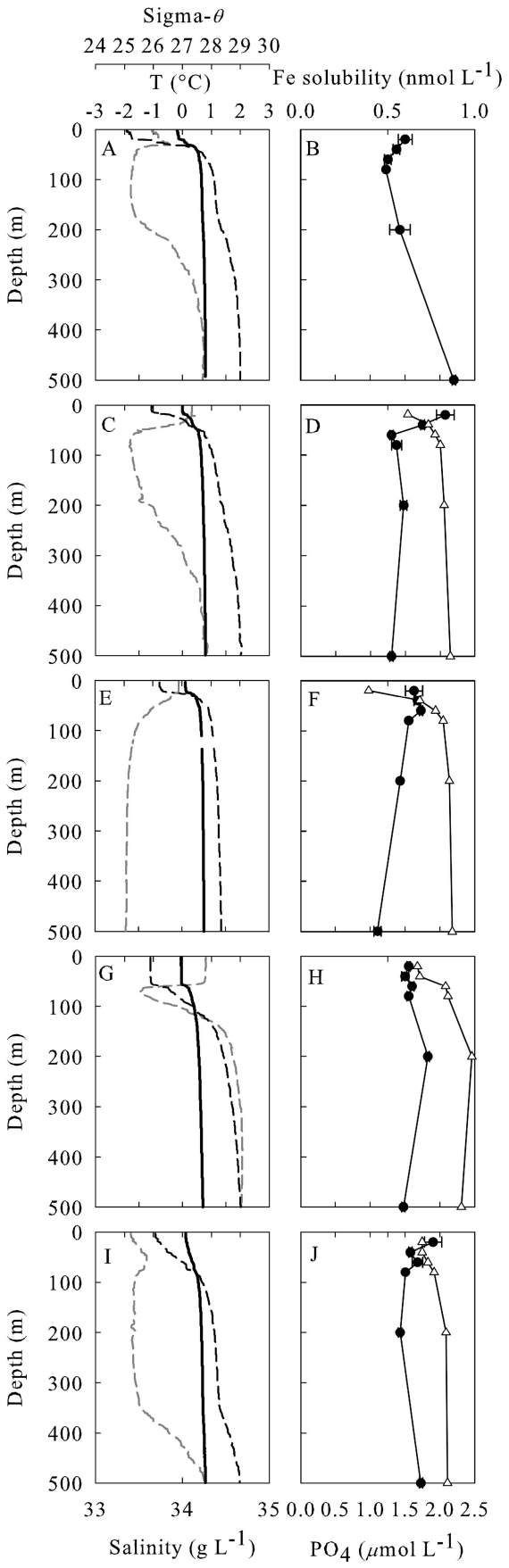


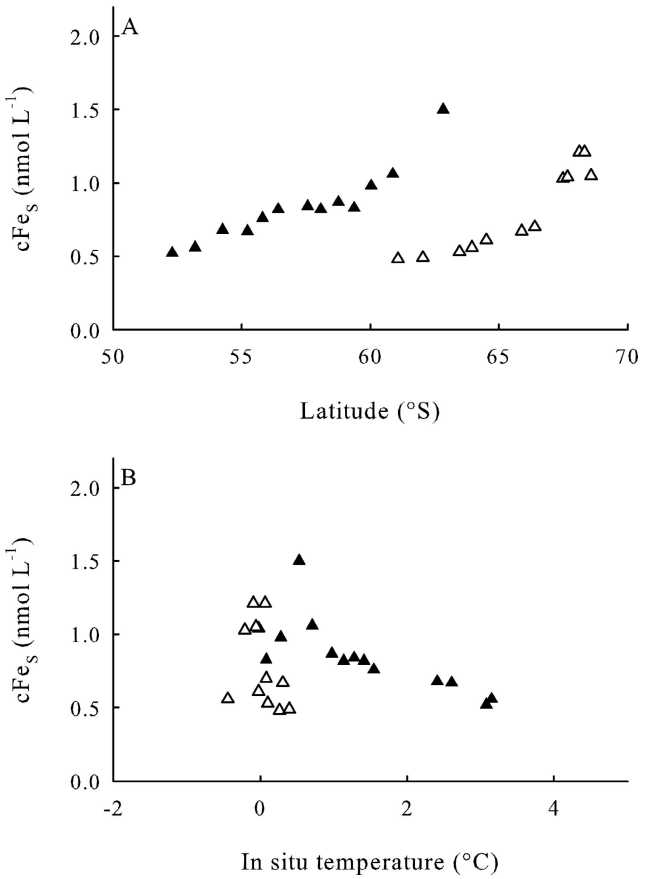


Fig. 5. A closer view of $cFe_S$ vs. (A) latitude and (B) temperature for the samples between the ice shelf and the Polar Front in the Weddell Sea (Coastal Zone; samples 13–2; white triangles) and for the samples between the SBACC and the Polar Front on the Kerguelen Plateau (Antarctic Zone; samples 25–37; black triangles).

northward (it is difficult to ascertain) but certainly did not show the striking pattern between fronts as observed for $cFe_S$ (Fig. 3A,D; Table 1). How much of a problem this presents is not clear, though, given that the dissolved Fe ligand measurement groups together the ligands in the soluble and in the colloidal phase, while the "organic" portion of Fe solubility is affected by ligands only in the soluble size fraction.

*$cFe_S$ in depth profiles*—Patterns of $cFe_S$ in the depth profiles (Fig. 4) also do not definitively support the notion that Fe solubility in the Southern Ocean is linked to organic matter remineralization; $cFe_S$ was highest toward the surface rather than at the deeper depths of 200 or 500 m in profiles 3, 4, and 6, and in none of the profiles is there a

←

Fig. 4. Data from the depth profiles (A, B) CTD 1, (C, D) CTD 3, (E, F) CTD 4, (G, H) CTD 5, and (I, J) CTD 6. (A, C, E, G, I) show salinity (black dashed line), temperature (gray dashed line), and sigma θ (bold line). (B, D, F, H, J) show $cFe_S$ (black circles) and concentrations of phosphate (white triangles).

sizable maximum at depth. This is in stark contrast to phosphate concentrations, which showed surface minima followed by a rapid increase toward deep maxima, a classic picture of utilization in the surface and regeneration with depth.

These results also stand in stark contrast to the results of Schlosser and Croot (2009) in the Mauritanian upwelling zone, where $cFe_S$ clearly increased with depth and phosphate concentration ($cFe_S = 0.68([PO_4]) + 0.46$; $R^2 = 0.77$; $n = 9$). The correlation between dissolved phosphate concentrations and $cFe_S$ in the water column was related to the release or activation of soluble ligands during the decomposition of particulate organic matter. For the ANTXXIII/9 data set presented here and as discussed earlier, there was no relationship between the phosphate and $cFe_S$ (Figs. 3, 4). This held for the depth profiles ($cFe_{S,org} = -0.09([PO_4]) + 0.65$; $R^2 = 0.11$; $n = 24$), for surface water data as a whole ($cFe_{S,org} = -0.01([PO_4]) + 0.76$; $R^2 = 0.02$; $n = 52$), and for just the subantarctic and subtropical portions of the data set ($cFe_{S,org} = 0.23([PO_4]) + 0.29$; $R^2 = 0.24$; $n = 12$).

They also differ from the picture from fluorescent dissolved organic matter (FDOM) further east in the Southern Ocean (Yamashita et al. 2007). The surface minimum of phosphate and FDOM is related to biological uptake and photodegradation (Chen and Bada 1992), respectively. The increase of both substances with depth is related to the remineralization of DOM (Yamashita et al. 2007). It should be noted, though, that much of the relationship between the two in Yamashita et al. (2007) was driven by the contrast between the lower values found in the upper 1000 m and the notably higher values of the Lower Circumpolar Deep Water and Southern Bottom Water, water masses that were not reached with the shallower sampling during ANTXXIII/9, especially in the vicinity of Prydz Bay (Nunes Vaz and Lennon 1996), where most of the water column profiles were taken (Fig. 1).

Surface and shallow subsurface (first 500 m) water masses in the Southern Ocean, between the SBACC and the PF, are strongly influenced by upwelling of very old, macronutrient-rich, and Fe-depleted water masses from 1000-m depth and deeper (Butzin et al. 2005). Most of the materials dissolved in these water masses have been there for a long time and not added recently by biological processes. The $> 2$ $\mu$mol $L^{-1}$ phosphate that comes from upwelling may be obscuring the use of phosphate concentrations in the Southern Ocean as a proxy for the recent addition of soluble organic ligands through organic matter decomposition in the upper ocean.

*Fe solubility due to organic ligands ($cFe_{S,org}$)*—Values of $cFe_S$ measured in the laboratory at room temperature (20°C) are the sum of two difference sources of Fe solubility: that due to ligands (the organic solubility, $cFe_{S,org}$) and that due to inorganic Fe solubility at 20°C. There is a reasonably well accepted model for calculating inorganic Fe solubility (Liu and Millero 2002), and this model has been supported by direct measurements of inorganic Fe solubility made between 5°C and 50°C on UV-irradiated seawater. It is thus in principle possible to subtract out the inorganic solubility of Fe at the measurement temperature of 20°C (0.155 nmol $L^{-1}$ at pH 7.8 according to Liu and Millero [2002] and Bellerby et al. [1995]) from $cFe_S$ to yield an estimate of Fe solubility in the samples due strictly to soluble organic ligands. The resulting values for $cFe_{S,org}$ range from 0.3 to 1.3 nmol $L^{-1}$ (Figs. 3, 6B; Table 2).

One question that can be addressed with the $cFe_{S,org}$ data is whether there is a discernible relationship between $cFe_{S,org}$ and concentrations of Fe-binding ligands in the dissolved size fraction. In the 28 samples for which both measurements were made (Table 1), $cFe_{S,org}$ represented 42 $\pm$ 26% of the concentration of dissolved Fe ligands (Table 2). These values ranged from 10% to 100%, but only in 6 of the 28 samples was $cFe_{S,org}$ greater than 54% of the dissolved ligand concentration (Fig. 6D). Of these six samples, the five with the highest values (samples 22, 24, 25, 26, and 27) were collected to the east of Prydz Bay near the SBACC. Leaving these five samples out reduces $cFe_{S,org}$ to being on average 32 $\pm$ 14% of the dissolved ligand concentration.

If the value of $cFe_{S,org}$ is equal to the total concentration of Fe-binding ligands in the soluble size fraction, then generally about 30% of the dissolved Fe ligands must have been in the soluble phase during ANTXXIII/9, leaving 70% of the dissolved ligands to have occurred in the colloidal size fraction. This is slightly lower than the estimate of 50–70% occurring as ligands that has been made from direct measurements of concentrations of soluble and colloidal Fe ligands (Boyé et al. 2010).

The four most anomalously high values of $cFe_{S,org}$ relative to dissolved ligand concentrations, those ranging from 61% to 100% that occurred to the east of Prydz Bay, near the Antarctic Divergence and SBACC, were high because relatively high concentrations of $cFe_{S,org}$ (0.86–1.38 nmol $L^{-1}$) coincided with relatively low concentrations of dissolved ligands (0.94–1.34 nmol $L^{-1}$). Concentrations of Chl *a* in these samples were also not notably high (0.07–0.24 $\mu$g $L^{-1}$), suggesting that solubility here may have its origins in water upwelled at the Antarctic Divergence rather than through high levels of biological activity at the surface, as mentioned in the previous section. In either case, if $cFe_{S,org}$ can be taken to reflect the concentration of Fe ligands in the soluble size fraction, then the balance between soluble and colloidal ligands may at times be heavily skewed toward the soluble. If that is true, then perhaps exposure at the surface results not only in the consumption or degradation of soluble ligands but also in their coagulation into colloids. It should be noted that the potentially significant impact of differences in pH from sample to sample on the measured values of $cFe_S$ and the associated values of $cFe_{S,org}$ could not be addressed because pH values at 20°C were unfortunately not determined as part of this data set.

*Fe solubility and in situ temperature*—Because of practical limitations, all values of Fe solubility ($cFe_S$) that have been published to date have been measured at room temperature ($\sim$ 20°C) rather than at the in situ temperature of the ocean water from which the samples were taken. This practice has worked reasonably well for samples of tropical

Table 2. Calculated and adjusted values related to $cFe_S$ for surface and water column samples from ANTXXIII/9.

| No. | $cFe_S$ (nmol $L^{-1}$) | $cFe_{S,org}$ (nmol $L^{-1}$) | $cFe_{S,org} \div L$ | $cFe_{S,adj}$ (nmol $L^{-1}$) |
|---|---|---|---|---|
| 1 | 0.614 | 0.459 | | 0.864 |
| 2 | 0.481 | 0.326 | | 0.864 |
| 3 | 0.487 | 0.332 | | 0.863 |
| 4 | 0.532 | 0.377 | 0.126 | 0.923 |
| 5 | 0.557 | 0.402 | | 0.976 |
| 6 | 0.608 | 0.453 | 0.103 | 1.006 |
| 7 | 0.671 | 0.516 | 0.168 | 1.052 |
| 8 | 0.696 | 0.541 | | 1.088 |
| 9 | 1.031 | 0.876 | | 1.438 |
| 10 | 1.035 | 0.880 | | 1.433 |
| 11 | 1.214 | 1.059 | | 1.607 |
| 12 | 1.211 | 1.056 | | 1.612 |
| 13 | 1.046 | 0.891 | 0.439 | 1.446 |
| CTD 1 | 0.596 | 0.441 | | 1.039 |
| | 0.545 | 0.390 | | 1.024 |
| | 0.504 | 0.349 | | 0.992 |
| | 0.486 | 0.331 | | 0.997 |
| | 0.573 | 0.418 | | 1.031 |
| | 0.882 | 0.727 | | 1.244 |
| CTD 3 | 0.830 | 0.675 | | 1.210 |
| | 0.704 | 0.549 | | 1.114 |
| | 0.522 | 0.367 | | 1.011 |
| | 0.554 | 0.399 | | 1.049 |
| | 0.591 | 0.436 | | 1.052 |
| | 0.520 | 0.365 | | 0.877 |
| 14 | 0.710 | 0.555 | | 1.108 |
| 14b | | | | |
| 15 | 0.857 | 0.702 | | 1.241 |
| 16 | 0.566 | 0.411 | | 0.968 |
| CTD 4 | 0.654 | 0.499 | | 1.056 |
| | 0.666 | 0.511 | | 1.087 |
| | 0.686 | 0.531 | | 1.141 |
| | 0.617 | 0.462 | | 1.091 |
| | 0.568 | 0.413 | | 1.068 |
| | 0.439 | 0.284 | | 0.945 |
| CTD 5 | 0.620 | 0.465 | | 0.978 |
| | 0.604 | 0.449 | | 0.962 |
| | 0.645 | 0.490 | | 1.074 |
| | 0.616 | 0.461 | | 1.080 |
| | 0.730 | 0.575 | | 1.048 |
| | 0.592 | 0.437 | | 0.897 |
| 17 | 0.597 | 0.442 | | 0.952 |
| 18 | 0.872 | 0.717 | 0.217 | 1.226 |
| 19 | 0.957 | 0.802 | 0.590 | 1.321 |
| 20 | 0.672 | 0.517 | 0.290 | 1.061 |
| 21 | 0.703 | 0.548 | 0.164 | 1.089 |
| 22 | 1.061 | 0.906 | 0.774 | 1.442 |
| 23 | 1.116 | 0.961 | 0.343 | 1.485 |
| CTD 6 | 0.756 | 0.601 | | 1.245 |
| | 0.628 | 0.473 | | 1.101 |
| | 0.665 | 0.510 | | 1.129 |
| | 0.595 | 0.440 | | 1.073 |
| | 0.570 | 0.415 | | 1.055 |
| | 0.686 | 0.531 | | 1.047 |
| 24 | 1.080 | 0.925 | 0.609 | 1.464 |
| 25 | 1.496 | 1.341 | 1.001 | 1.867 |
| 26 | 1.056 | 0.901 | 1.060 | 1.418 |
| 27 | 0.976 | 0.821 | 0.892 | 1.359 |
| 28 | 0.830 | 0.675 | 0.540 | 1.222 |
| 29 | 0.868 | 0.713 | 0.427 | 1.218 |
| 30 | 0.817 | 0.662 | | 1.159 |
| 31 | 0.843 | 0.688 | 0.513 | 1.179 |
| 32 | 0.815 | 0.660 | 0.273 | 1.145 |
| 33 | 0.758 | 0.603 | | 1.082 |
| 34 | 0.675 | 0.520 | 0.195 | 0.956 |
| 35 | 0.679 | 0.524 | 0.285 | 0.967 |
| 36 | 0.565 | 0.410 | | 0.825 |
| 37 | 0.518 | 0.363 | 0.211 | 0.781 |
| 38 | 0.726 | 0.571 | | 0.960 |
| 38b | | | | |
| 39 | 0.850 | 0.695 | 0.331 | 1.076 |
| 40 | 0.772 | 0.617 | | 0.982 |
| 41 | 0.915 | 0.760 | 0.251 | 1.108 |
| 42 | 0.738 | 0.583 | | 0.924 |
| 43 | 0.886 | 0.731 | | 1.058 |
| 44 | 0.848 | 0.693 | 0.444 | 1.013 |
| 45 | 0.876 | 0.721 | 0.530 | 0.998 |
| 46 | 0.775 | 0.620 | | 0.893 |
| 47 | 0.792 | 0.637 | 0.455 | 0.938 |
| 48 | 0.599 | 0.444 | | 0.687 |
| 49 | 0.638 | 0.483 | 0.293 | 0.686 |
| 50 | 0.667 | 0.512 | | 0.691 |
| 51 | 0.565 | 0.410 | 0.261 | 0.542 |

surface seawater that have in situ temperatures in the neighborhood of 20–25°C. However, it appears more difficult for total Fe solubility of samples of water whose in situ temperature was below 20°C. This is because the measurement of $cFe_S$ yields the sum of the organic solubility (that which is due to ligands) and the inorganic solubility (that which is related to non–ligand-bound Fe), and inorganic solubility varies strongly with temperature (Liu and Millero 1999, 2002). Inorganic Fe solubility, for example, should increase approximately threefold as temperature drops from 20°C to 5°C (Liu and Millero 1999, 2002). Thus, the total capacity of samples with low in situ temperatures for soluble Fe will be underestimated if total Fe solubility is measured in the lab at 20°C. That this is the case is very clear from the fact that the bulk of the values of $cFe_S$ in the ANTXXIII/9 data set are lower than that calculated for inorganic Fe solubility by the model of Liu and Millero (2002) (Fig. 7A).

It is worth noting that $cFe_{S,org}$ in the Southern Ocean samples from south of the PF tends to be lower than the modeled inorganic Fe solubility (Fig. 7B) but that this is not true of samples from the subantarctic or the subtropics from the same cruise, nor is it true for most of the tropical Atlantic samples of Schlosser and Croot (2009). This difference is tied to the high values for inorganic Fe solubility expected at lower temperatures by both the model of Liu and Millero (2002) and real measurements. One might predict from the higher inorganic Fe solubility at lower temperatures that Fe-binding ligands are much more critical to Fe availability and Fe residence time in warmer waters than in cooler ones.

Interestingly, not only does inorganic Fe solubility decrease with increasing temperature (Liu and Millero

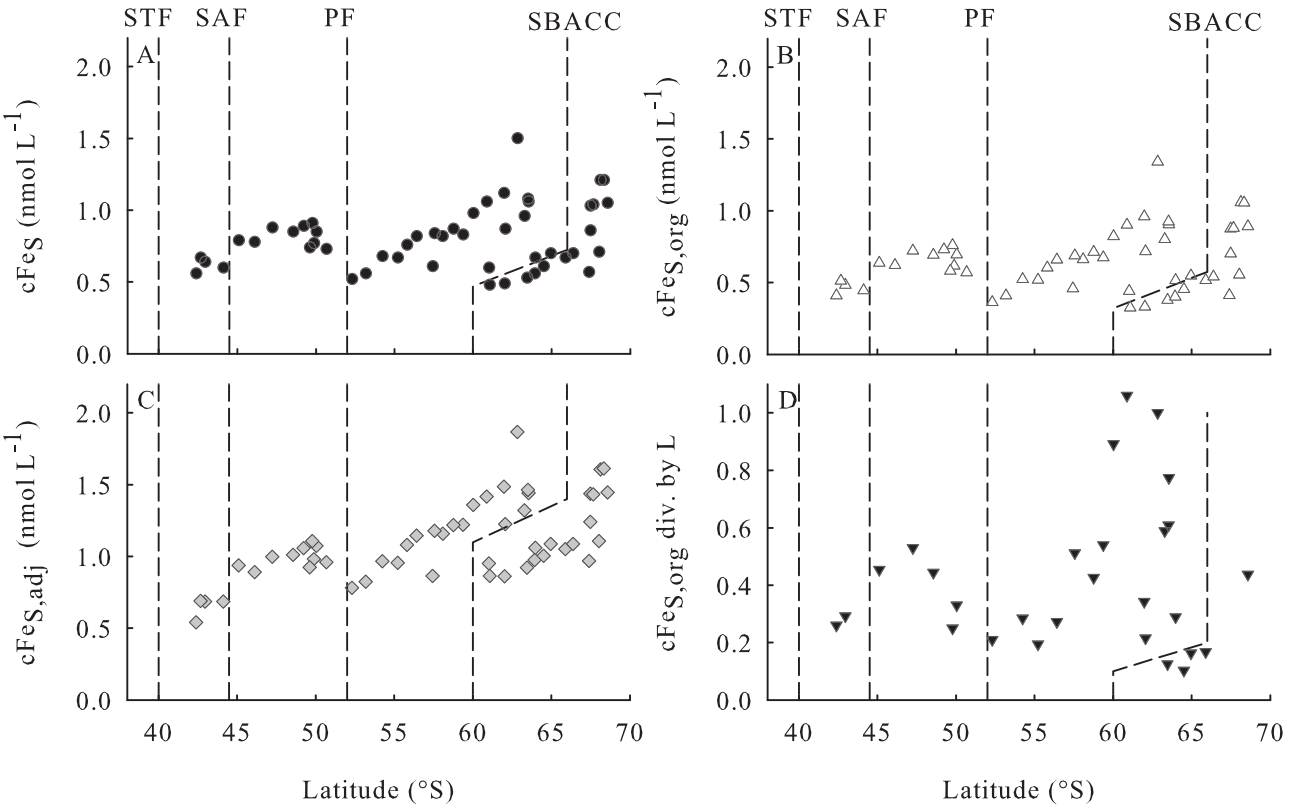


Fig. 6. Calculated estimates from the surface samples: (A) $cFe_S$, (B) $cFe_{S,org}$, (C) $cFe_{S,adj}$, and (D) $cFe_{S,org}$ divided by dissolved ligand concentration. Dashed lines indicate the different Antarctic fronts as in Fig. 3.

2002), but it appears that $cFe_{S,org}$ can as well. The $cFe_{S,org}$ of samples from the subantarctic and subtropical locations of ANTXXIII/9 (Fig. 7B) fall along a straight line vs. in situ temperature with samples from the Mauritanian upwelling zone in the tropical Atlantic (Schlosser and Croot 2009; $cFe_{S,org} = -0.03T + 0.84$; $R^2 = 0.83$; $n = 35$). The reasons for such a decline in $cFe_{S,org}$ with increasing in situ temperature are not clear. There may be a greater proportion of dissolved Fe-binding ligands in the colloidal size fraction at higher temperatures. It may be that soluble ligand concentrations are lower at higher temperatures because of higher rates of decomposition of ligands at higher temperatures, or it may be that in situ temperatures are influencing the measurement of $cFe_{S,org}$ in a way that is not yet understood.

That the measured (organic + inorganic) Fe solubility is lower than the expected value for inorganic solubility alone means that $cFe_S$ does not represent the total Fe solubility of samples that had in situ temperatures significantly less than 20°C. One way of correcting for the discrepancy would be to add back to $cFe_{S,org}$ the inorganic solubility calculated for the in situ temperature (Liu and Millero 1999) and in situ pH (pH 8.0; Bellerby et al. 1995), an adjusted value we have termed $cFe_{S,adj}$ (Table 2; Figs. 6C, 7C). The temperature adjustment, however, is best done on seawater samples where the in situ temperature was above 5°C (as this falls within the range of the solubility model that was constrained by measurements) and can only cautiously be applied to those samples with in situ temperatures below 5°C (the gray domains on Fig. 7). In this region, the equations of Liu and Millero (2002) provide only an extrapolation.

Such an adjustment assumes two things: that the Fe solubility due to soluble organic ligands does not change with temperature and that the model for inorganic Fe solubility without any in situ pH correction and temperature-driven crystalline phase transition of solid Fe phases is sufficiently correct. However, Fe solubility due to soluble organic ligands may possibly change with temperature because log $K_{FeL}$ may vary with temperature (Liu and Millero 2002), although there are few data that could be used to address the binding strength of soluble organic Fe ligands with changing temperatures. Voltammetric measurements (data not shown) on 0.2-$\mu$m filtered seawater samples have shown that iron ligand concentrations and the conditional stability constant of organically complexed Fe do not greatly differ between 4°C and 20°C. Regarding the second point, the model of inorganic Fe solubility of Liu and Millero (2002), to the extent that it has been tested, appears robust. However, the model has not been ground truthed below 5°C, and it is possible that the method used for testing overestimated the solubility with its approach. This uncertainty should be solved with further measurements of inorganic Fe solubility that are made across a spectrum of temperatures from high (~ 40°C) to low (the freezing point) for each single sample of UV-irradiated seawater. Another

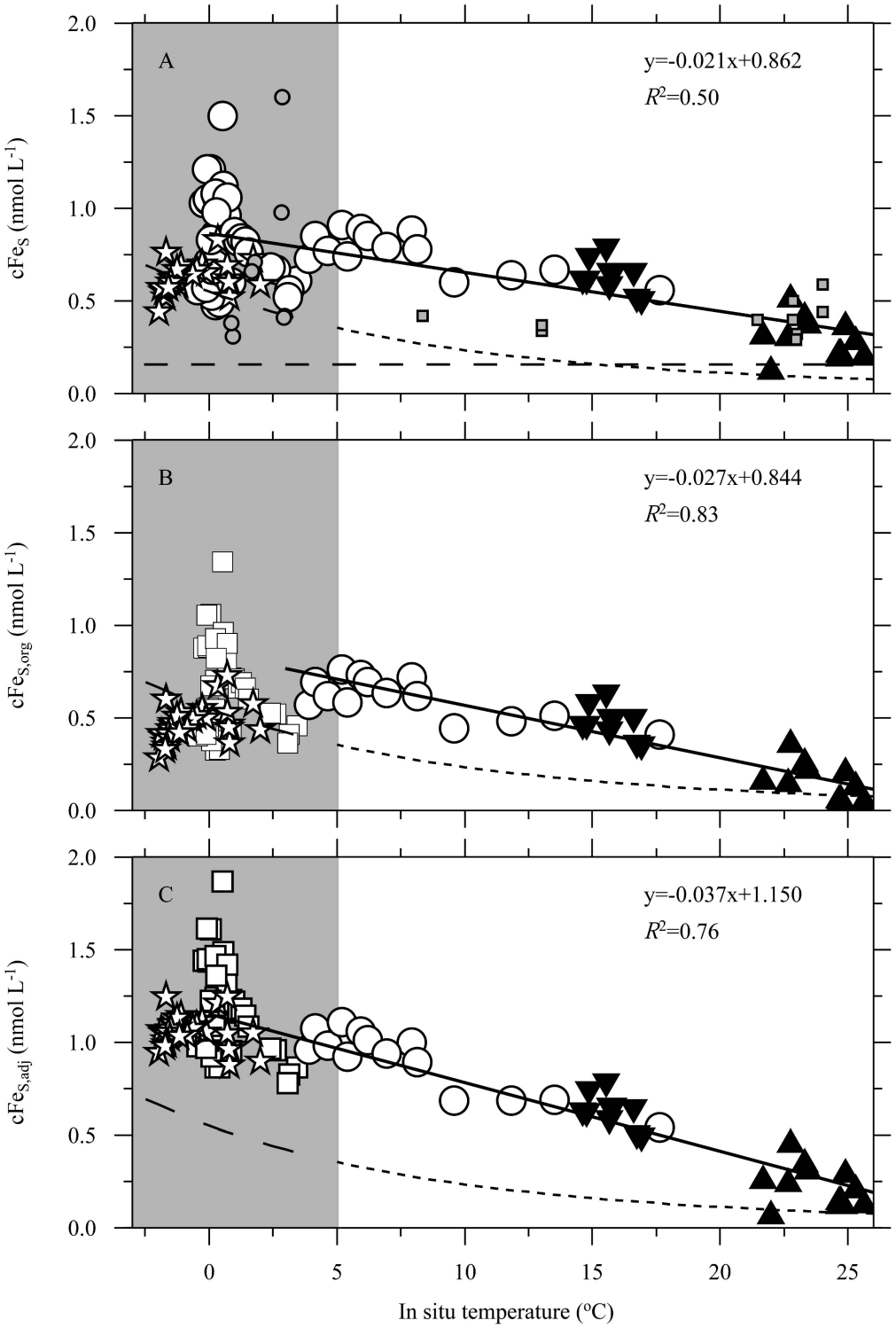


Fig. 7. (A) Measured Fe solubility ($cFe_S$), (B) organic Fe solubility ($cFe_{S,org}$), and (C) adjusted total in situ Fe solubility ($cFe_{S,adj}$) vs. in situ temperature. Data shown in white are from ANTXXIII/9 (squares: surface samples from south of the Polar Front; stars: depth profile samples; circles: subantarctic and subtropical samples) and from cruise M68-3 (Schlosser and Croot 2009) in the Mauritanian upwelling zone in the tropical Atlantic (filled triangles: surface samples; inverted filled triangles: depth profiles). (A) Smaller gray symbols indicate published Fe solubility data of surface seawaters (5–20 m) measured by Kuma et al. (1996; gray squares) and Tani et al. (2003; gray circles). The long-dashed line shows the inorganic Fe solubility in the samples at measurement temperature (20°C and pH 7.8 ≈ 0.155 nmol $L^{-1}$; Liu and Millero 1999, 2002). (A–C) The dashed black curves show the total inorganic Fe solubility calculated from the model of Liu and Millero (2002) for pH 8. The gray domain indicates the temperature range over which this calculation is an extrapolation.

issue that enters the equations of the model is the in situ pH. By the lack of in situ pH measurements at sea, we were forced to use a fixed, estimated value for the in situ pH. This simplified assumption of an unchanging pH has been made because slight changes of pH when pH is near 8 only drive minor changes in inorganic Fe solubility at both 20°C (e.g., pH 8–8.1 yields a change of 0.015 nmol $L^{-1}$) and 5°C (pH 8 to pH 8.1 yields a change of 0.095 nmol $L^{-1}$) when compared to in situ temperature.

The only alternative to this proposed adjustment would be to make future measurements of total Fe solubility at in situ temperatures (by conducting the solubility incubations in controlled-temperature baths or cold rooms), something that would be inconvenient for depth profiles.

Because inorganic Fe solubility is predicted to be high at low temperatures, such as occur in the Southern Ocean, values of adjusted in situ Fe solubility ($cFe_{S,adj}$) in the ANTXXIII/9 samples were generally more than 1.5 times larger than $cFe_{S,org}$ (Table 2; Figs. 6, 7). As mentioned previously, this implies that inorganic Fe solubility is a much more important regulator of total Fe solubility in these cooler waters than it is in warmer waters. It also suggests that if it is important for organisms for Fe to be retained in the soluble size fraction, there is much less pressure on them in cooler waters to excrete Fe-binding ligands. That would imply that a large portion of dissolved Fe in deep and bottom waters as well as Fe in cooler waters in the surface need not necessarily be organically complexed (e.g., after dust deposition) to remain more bioavailable (i.e., soluble) or to extend the residence time of Fe in seawater. For example, dissolved Fe concentrations in deep and bottom waters (> 3000 m) of the North Atlantic Ocean range between 0.7 and 0.8 nmol $L^{-1}$ at temperatures of ~ 2°C (Laes et al. 2003). Using the above model, more than half of the dissolved Fe at these depths (0.45 nmol $L^{-1}$) could be stable in the inorganic soluble form, although that seems unrealistic, given the large amount of acid-dissolvable Fe (several nmol $L^{-1}$; Ezoe et al. 2004) and the excess of organic ligands (~ 2 nmol $L^{-1}$; Boyé et al. 2006) coexisting in equilibrium at these depths.

Somewhat intriguingly, when the solubility values are adjusted for in situ Fe solubility, the Antarctic samples from ANTXXIII/9 now fall in line vs. in situ temperature with the subantarctic and subtropical samples from ANTXXIII/9 and the samples from the tropical Atlantic (Schlosser and Croot 2009; $cFe_{S,adj} = -0.037T + 1.150$; $R^2 = 0.76$; $n = 86$; Fig. 7C), whereas without this adjustment, the Antarctic samples as a whole did not fall in line (Fig. 7B). It is not clear what this implies.

However, because inorganic Fe solubility calculated by the model of Liu and Millero (2002) decreases nonlinearly with in situ temperature, similar curvature would be expected for the relationship between $cFe_{S,adj}$ and temperature (Fig. 7C). This is clearly not the case, and the linear correlation may be spurious, driven by the large temperature effect on inorganic Fe solubility at low temperatures. Alternatively, the line in Fig. 7C may hint at something that is real but that remains to be investigated, such as the effect of temperature-dependent variability in the DOM pool postulated in the previous section. Whatever the case, further inquiry into this relationship is warranted to determine whether it holds over a larger set of samples and ocean regions and, if so, what the mechanisms behind it are.

*Acknowledgments*

We thank the captain and crew of the R/V *Polarstern* (ANTXXIII/9) and the anonymous reviewers who provided constructive comments on the manuscript. This work was supported by the Deutsche Forschungsgemeinschaft (DFG)-Schwerpunktprogramm 1158 Anarktisforschung via grants awarded to PC (CR145/5-1 and CR145/11-1) and CDLR (DE1455/1-1).

## References

Baker, A. R., and P. L. Croot. 2010. Atmospheric and marine controls on aerosol iron solubility in seawater. Mar. Chem. **120:** 4–13, doi:10.1016/j.marchem.2008.09.003

Barbeau, K. 2006. Photochemistry of organic Fe(III) complexing ligands in oceanic systems. Photochem. Photobiol. **82:** 1505–1516.

Bellerby, R. G. J., D. R. Turner, and J. E. Robertson. 1995. Surface pH and pC02 distributions in the Bellingshausen Sea, Southern Ocean, during the early Austral summer. Deep-Sea Res. II **42:** 1093–1107, doi:10.1016/0967-0645(95)00068-2

Boyd, P. W. 2002. The role of iron in the biogeochemistry of the Southern Ocean and equatorial Pacific: A comparison of in situ iron enrichments. Deep-Sea Res. II **49:** 1803–1821, doi:10.1016/S0967-0645(02)00013-9

———, E. Ibisanmi, S. G. Sander, K. A. Hunter, and G. A. Jackson. 2010. Remineralization of upper ocean particles: Implications for iron biogeochemistry. Limnol. Oceanogr. **55:** 1271–1288, doi:10.4319/lo.2010.55.3.1271

Boyé, M., and others. 2006. The chemical speciation of iron in the north-east Atlantic Ocean. Deep-Sea Res. I **53:** 667–693, doi:10.1016/j.dsr.2005.12.015

———, and ———. 2010. Significant portion of dissolved organic Fe complexes in fact is Fe colloids. Mar. Chem. **122:** 20–27, doi:10.1016/j.marchem.2010.09.001

Brown, J., A. Colling, D. Park, J. Phillips, D. Rothery, and J. Wright. 1989. Ocean water masses, p. 172–185. *In* G. Bearman [ed.], Ocean circulation. Pergamon Press.

Bruland, K. W., R. P. Franks, G. A. Knauer, and J. H. Martin. 1979. Sampling and analytical methods for the determination of copper, cadmium, zinc, and nickel at the nanogram per liter level in sea water. Anal. Chim. Acta **105:** 233–245, doi:10.1016/S0003-2670(01)83754-5

Butzin, M., M. Prange, and G. Lohmann. 2005. Radiocarbon simulations for the glacial ocean: The effects of wind stress, Southern Ocean sea ice and Heinrich events. Earth Planet. Sci. Lett. **235:** 45–61.

Chen, R. F., and J. L. Bada. 1992. The fluorescence of dissolved organic matter in seawater. Mar. Chem. **37:** 191–221, doi:10.1016/0304-4203(92)90078-O

Covington, A. K., M. I. A. Ferra, and R. A. Robinson. 1977. Ionic product and enthalpy of ionization of water from electromotive force measurements. J. Chem. Soc. Faraday Trans. 1 **73:** 1721–1730, doi:10.1039/f19777301721

Croot, P. L., K. Andersson, M. Öztürk, and D. Turner. 2004*a*. The distribution and speciation of iron along 6° E, in the Southern Ocean. Deep-Sea Res. II **51:** 2857–2879, doi:10.1016/j.dsr2.2003.10.012

———, and M. Johansson. 2000. Determination of iron speciation by cathodic stripping voltammetry in seawater using the competing ligand 2-(2-thiazolylazo)-p-cresol (TAC).

Electroanalysis **12:** 565–576, doi:10.1002/(SICI)1521-4109(200005)12:8<565::AID-ELAN565>3.0.CO;2-L

———, P. Streu, and A. R. Baker. 2004*b*. Short residence time for iron in surface seawater impacted by atmospheric dry deposition from Saharan dust events. Geophys. Res. Lett. **31:** 1–4.

Danielsson, L.-G., B. Magnusson, and S. Westerlund. 1978. An improved metal extraction procedure for the determination of trace metals in sea water by atomic absorption spectrometry with electrothermal atomization. Anal. Chim. Acta **98:** 47–57, doi:10.1016/S0003-2670(01)83237-2

Ezoe, M., T. Ishita, M. Kinugasa, X. Lai, K. Norisuye, and Y. Sohrin. 2004. Distributions of dissolved and acid-dissolvable bioactive trace metals in the North Pacific Ocean. Geochem. J. **38:** 535–550, doi:10.2343/geochemj.38.535

Gobler, C. J., D. A. Hutchins, N. S. Fisher, E. M. Cosper, and S. A. Sanudo-Wilhelmy. 1997. Release and bioavailability of C, N, P, Se, and Fe following viral lysis of a marine chrysophyte. Limnol. Oceanogr. **42:** 1492–1504, doi:10.4319/lo.1997.42.7.1492

Grasshoff, K., M. Erhardt, and K. Kremling. 1999. Methods of seawater analysis, 3rd ed. Wiley-VCH.

Heil, P., and I. Allison. 1999. The pattern and variability of Antarctic sea-ice drift in the Indian Ocean and western Pacific sectors. J. Geophys. Res. **104:** 15789–15802, doi:10.1029/1999JC900076

Helmers, E., L. Mart, and O. Schrems. 1991. Lead in Atlantic surface waters as a tracer for atmospheric input. Fresenius J. Anal. Chem. **340:** 580–584, doi:10.1007/BF00322433

Kuma, K., J. Nishioka, and K. Matsunaga. 1996. Controls on iron(III) hydroxide solubility in seawater: The influence of pH and natural organic chelators. Limnol. Oceanogr. **41:** 396–407, doi:10.4319/lo.1996.41.3.0396

Laes, A., S. Blain, P. Laan, E. P. Achterberg, G. Sartou, and H. J. W. De Baar. 2003. Deep dissolved iron profils in the eastern North Atlantic in relation to water masses. Geophys. Res. Lett. **30:** 1–8, doi:10.1029/2003GL017902

Liu, H., and F. J. Millero. 1999. The solubility of iron hydroxide in sodium chloride solutions. Geochim. Cosmochim. Acta **63:** 3487–3497, doi:10.1016/S0016-7037(99)00270-7

———, and ———. 2002. The solubility of iron in seawater. Mar. Chem. **77:** 43–54, doi:10.1016/S0304-4203(01)00074-3

Martin, J. H. 1990. Glacial-interglacial CO2 change: The iron hypothesis. Paleoceanography **5:** 1–11, doi:10.1029/PA005i001p00001

Martinez, J. S., G. P. Zhang, P. D. Holt, H.-T. Jung, C. J. Carrano, M. G. Haygood, and A. Butler. 2000. Self-assembling amphiphilic siderophores from marine bacteria. Science **287:** 1245–1247, doi:10.1126/science.287.5456.1245

Nakabayashi, S., K. Kuma, K. Sasaoka, S. Saitoh, M. Mochizuki, N. Shiga, and M. Kusakabe. 2002. Variation in iron(III) solubility and iron concentration in the northwestern North Pacific Ocean. Limnol. Oceanogr. **47:** 885–892, doi:10.4319/lo.2002.47.3.0885

Nishioka, J., S. Takeda, H. J. W. de Baar, P. L. Croot, M. Boyé, P. Laan, and K. R. Timmermans. 2005. Changes in the concentration of iron in different size fractions during an iron enrichment experiment in the open Southern Ocean. Mar. Chem. **95:** 51–63, doi:10.1016/j.marchem.2004.06.040

Nunes Vaz, R. A., and G. W. Lennon. 1996. Physical oceanography of the Prydz Bay region of Antarctic Waters. Deep-Sea. Res. I **43:** 603–641, doi:10.1016/0967-0637(96)00028-3

Orsi, A. H., W. D. Nowlin, Jr, and T. Whitworth, III. 1993. On the circulation and stratification of the Weddell Gyre. Deep-Sea Res. I **40:** 169–203, doi:10.1016/0967-0637(93)90060-G

Phinney, J. T., and K. W. Bruland. 1994. Uptake of lipophilic organic Cu, Cd, and Pd complexes in the coastal diatom *Thalassiosira weissflogii*. Environ. Sci. Technol. **28:** 1781–1790, doi:10.1021/es00060a006

Rue, E. L., and K. W. Bruland. 1997. The role of organic complexation on ambient iron chemistry in the equatorial Pacific Ocean and the response of a mesoscale iron addition experiment. Limnol. Oceanogr. **42:** 901–910, doi:10.4319/lo.1997.42.5.0901

Sato, M., S. Takeda, and K. Furuya. 2007. Iron regeneration and organic iron(III)-binding ligand production during in situ zooplankton grazing experiment. Mar. Chem. **106:** 471–488, doi:10.1016/j.marchem.2007.05.001

Schlosser, C., and P. L. Croot. 2008. Application of cross-flow filtration for determining the solubility of iron species in open ocean seawater. Limnol. Oceanogr.: Methods **6:** 630–642, doi:10.4319/lom.2008.6.630

———, and ———. 2009. Controls on seawater Fe(III) solubility in the Mauritanian upwelling zone. Geophys. Res. Lett. **36:** 1–5, doi:10.1029/2009GL038963

Shaked, Y., A. B. Kustka, and F. M. M. Morel. 2005. A general kinetic model for iron acquisition by eukaryotic phytoplankton. Limnol. Oceanogr. **50:** 872–882, doi:10.4319/lo.2005.50.3.0872

Smith, N. R., D. Zhaoqian, K. R. Kerry, and S. Wright. 1984. Water masses and circulation in the region of Prydz Bay, Antarctica. Deep-Sea Res. **31:** 1121–1147.

Tani, H., J. Nishioka, K. Kuma, H. Takata, Y. Yamashita, E. Tanoue, and T. Midorikawa. 2003. Iron(III) hydroxide solubility and humic-type fluorescent organic matter in the deep water column of the Okhotsk Sea and the northwestern North Pacific Ocean. Deep-Sea Res. I **50:** 1063–1078, doi:10.1016/S0967-0637(03)00098-0

Tomczak, M., and J. S. Godfrey. 2003. Regional oceanography: An introduction, 2nd ed. Daya Publishing House.

Wagener, T., C. Guieu, R. Losno, S. Bonnet, and N. Mahowald. 2008. Revisiting atmospheric dust export to the Southern Hemisphere ocean: Biogeochemical implications. Glob. Biogeochem. Cycles **22:** 1–13, doi:10.1029/2007GB002984

Witter, A. E., and G. W. Luther. 1998. Variation in Fe-organic complexation with depth in the northwestern Atlantic Ocean as determined using a kinetic approach. Mar. Chem. **62:** 241–258, doi:10.1016/S0304-4203(98)00044-9

Yamashita, Y., A. Tsukaski, T. Nishida, and E. Tanoue. 2007. Vertical and horizontal distribution of fluorescent dissolved organic matter in the Southern Ocean. Mar. Chem. **106:** 498–509, doi:10.1016/j.marchem.2007.05.004

*Associate Editor: Mary I. Scranton*

*Received: 04 July 2011*
*Accepted: 15 November 2011*
*Amended: 30 November 2011*